# Hubbard Model for Atomic Impurities Bound by the Vortex Lattice of a Rotating Bose-Einstein Condensate

T. H. Johnson,[1,2,3] Y. Yuan,[4,5,6] W. Bao,[5,*] S. R. Clark,[7,3,†] C. Foot,[2] and D. Jaksch[2,1,3]
[1]Centre for Quantum Technologies, National University of Singapore, 117543 Singapore
[2]Clarendon Laboratory, University of Oxford, Parks Road, Oxford OX1 3PU, United Kingdom
[3]Keble College, University of Oxford, Parks Road, Oxford OX1 3PG, United Kingdom
[4]Beijing Computational Science Research Center, Beijing 100094, China
[5]Department of Mathematics, National University of Singapore, 119076 Singapore
[6]College of Mathematics and Computer Science, Synthetic Innovation Center for Quantum Effects and Applications, Hunan Normal University, Changsha, Hunan Province 410081, China
[7]Department of Physics, University of Bath, Claverton Down, Bath BA2 7AY, United Kingdom
(Received 1 January 2016; published 14 June 2016)

We investigate cold bosonic impurity atoms trapped in a vortex lattice formed by condensed bosons of another species. We describe the dynamics of the impurities by a bosonic Hubbard model containing occupation-dependent parameters to capture the effects of strong impurity-impurity interactions. These include both a repulsive direct interaction and an attractive effective interaction mediated by the Bose-Einstein condensate. The occupation dependence of these two competing interactions drastically affects the Hubbard model phase diagram, including causing the disappearance of some Mott lobes.

DOI: 10.1103/PhysRevLett.116.240402

Wherever vortices have been detected, there has been interest in particles bound inside them. For example, particles bound in the vortices of rotating superfluid helium [1–4] were used to count [5] and visualize [6–8] vortices, and determine their properties [9,10]. Meanwhile, bound particle-antiparticle pairs in vortex lattices of clean type-II superconductors [11] received theoretical [12–14] and experimental [15] attention for their role in charge transport [16] and relaxation.

In this Letter, we consider a vortex lattice of a rotating atomic Bose-Einstein condensate (BEC) [17–21] in which a small number of cold bosonic atoms, called impurities, are bound. Imbalanced cold atomic mixtures have been used to study the effect of the majority species on the transport of the impurities [22–25], often with an external lattice potential [26–28], and the formation of polarons [29–31]. Reference [32] considered the continuum modes of impurities immersed in a BEC vortex lattice, but not the regime in which the bound modes of impurities are important.

For this regime, we develop a Hubbard model description for the impurities. To account for strong repulsive interactions between impurities [33–42] and with bosons comprising the BEC [43–46], we allow the wave functions of particles at each site to depend on the number of impurities at that site, leading to an occupation-dependent Hubbard model [47]. Our system contrasts with typical experiments featuring cold atoms in rigid optical lattices. The soft vortex lattice makes the interaction of impurities with lattice degrees of freedom intrinsic to the system, similar to solid-state systems described by so-called dynamical Hubbard models [48–52]. In our setup the range of impurity-impurity interactions induced by this softness is restricted by the healing length $\xi$ [30]. In contrast, soft weak optical lattice potentials, e.g., created by driven cavities [53,54], induce longer-ranged interactions and noise [55], qualitatively different from our proposal.

We focus on the on-site interactions between impurities, which govern the strongly interacting part of the phase diagram. We find that the occupation dependence, in conjunction with competition between direct repulsive impurity-impurity interactions and effective attractive interactions mediated by the BEC [29,30], drastically alters the typical structure of the ground state phase diagram. We give an example in which low-occupation Mott lobes are missing entirely.

*System.*—Our system consists of a cold atomic mixture of two bosonic species $s = a, b$, which we call impurities and bosons, respectively. They have mass $m_s$ and rotate with frequency $\Omega$ around the $z$ axis. Both species are trapped sufficiently strongly along the $z$ axis that the system is governed by the two-dimensional Hamiltonian $\hat{H} = \sum_{s=a,b} \hat{H}_s + \hat{H}_{ab}$. For each species, in the rotating frame, we have [21]

$$\hat{H}_s = \int d\mathbf{r} \hat{\Psi}_s^\dagger(\mathbf{r}) \left( h_s(\mathbf{r}) + \frac{g_s}{2} \hat{\Psi}_s^\dagger(\mathbf{r}) \hat{\Psi}_s(\mathbf{r}) \right) \hat{\Psi}_s(\mathbf{r})$$

with the single-particle Hamiltonian

$$h_s(\mathbf{r}) = -\frac{\hbar^2 \nabla^2}{2m_s} + V_s(\mathbf{r}) + \Omega L_z(\mathbf{r}),$$

creation $\hat{\Psi}_s^\dagger(\mathbf{r})$ and annihilation $\hat{\Psi}_s(\mathbf{r})$ field operators, $L_z(\mathbf{r}) = -i\hbar\partial/\partial\phi$ for the $z$-axis angular momentum,

 

position vector $\mathbf{r}$ orthogonal to the $z$ axis, and azimuthal angle $\phi$. The repulsive density-density intra- and interspecies interactions have strengths $g_s$ and $g_{ab}$, respectively. Accordingly, the interspecies interaction Hamiltonian is

$$\hat{H}_{ab} = g_{ab} \int d\mathbf{r} \hat{\Psi}_a^\dagger(\mathbf{r}) \hat{\Psi}_a(\mathbf{r}) \hat{\Psi}_b^\dagger(\mathbf{r}) \hat{\Psi}_b(\mathbf{r}).$$

The relationship between the parameters of this effective two-dimensional system and those of the original three-dimensional system are given in Sec. I of the Supplemental Material [56].

For isotropic harmonic potentials $V_s(\mathbf{r}) = m_s \Omega_s^2 r^2/2$, the single-particle Hamiltonians can be rewritten

$$h_s(\mathbf{r}) = \frac{\Pi_s^2}{2m_s} + \frac{m_s}{2}(\Omega_s^2 - \Omega^2) r^2$$

with covariant momenta $\Pi_s = -i\hbar\nabla + m_s \mathbf{A}(\mathbf{r})$ and vector potential $\mathbf{A} = -\Omega \mathbf{r} \times \hat{\mathbf{z}}$ (symmetric gauge). We choose $\Omega \lesssim \Omega_s$, ensuring the system is trapped but nevertheless approximately homogeneous, $h_s(\mathbf{r}) \approx \Pi_s^2/2m_s$, in the bulk.

*Vortex lattice.*—We use a Gross-Pitaevskii mean-field treatment in which, at low temperatures, the $N_b$ bosons form a BEC with wave function $\psi^{\{0\}}(\mathbf{r})$. The result, found using the normalized gradient flow method via backward Euler Fourier pseudospectral discretization [57–59], is shown in Fig. 1(a). We consider the regime of large $\Omega$, in which the condensate exhibits singly quantized vortices whose centers $\mathbf{R}$ form an equilateral triangular lattice with nearest-neighbor distance $a = (2\pi\hbar/\sqrt{3} m_b \Omega)^{1/2}$ [21]. In the bulk of the condensate, the density $n^{\{0\}}(\mathbf{r}) = N_b |\psi^{\{0\}}(\mathbf{r})|^2$ of the bosons provides the impurities with a periodic potential $V_{ab}^{\{0\}}(\mathbf{r}) = g_{ab} n^{\{0\}}(\mathbf{r})$ with the same geometry as the vortex lattice. The vortex cores have a width of the order of the healing length $\xi = \hbar/\sqrt{g_b n_0 m_b}$ and depth $g_{ab} n_0$, where $n_0$ is the density of bosons away from the vortex cores. Unlike typical optical lattice potentials, the width $\xi$, depth $g_{ab} n_0$, and separation $a$ of potential wells can be controlled separately and are not limited by optical wavelengths. We consider large rotation energies on the order of interaction energies $\hbar\Omega \lesssim n_0 g_b/2$, so that the widths of the wells are similar to their separations $\xi \lesssim a$, and bosonic densities of roughly ten bosons per vortex, large enough that the mean-field Gross-Pitaevskii description holds [60,61].

*Hubbard physics.*—The impurities, a minority species $N_a < N_b$, are immersed in the vortex lattice. For large enough $g_{ab}$ or $m_a$, the impurities occupy bound localized states inside the potential wells of the vortex lattice. An example of this is shown in Fig. 1(b). A simple calculation for a Gaussian impurity in a finite circular well of width $\xi$ and depth $g_{ab} n_0$ gives an approximate condition $g_{ab}/g_b > m_b/2m_a$ for localization.

It follows that the low-energy dynamics of impurities consists of hopping between the bound states at vortex lattice sites, with many-body effects accounted for by the energy cost of impurities sharing the same site. A minimal physical description of such a system is illustrated in Fig. 1(c) and corresponds mathematically to a single-band Hubbard model with occupation-dependent parameters [47]

$$\hat{H}_{\text{Hubbard}} = E^{\{0\}} + \sum_{\mathbf{R}} \epsilon^{\{\hat{n}_\mathbf{R}\}} \hat{n}_\mathbf{R} + \sum_{\langle \mathbf{R}'\mathbf{R} \rangle} \hat{a}_{\mathbf{R}'}^\dagger J_{\mathbf{R}'\mathbf{R}}^{\{\hat{n}_{\mathbf{R}'} \hat{n}_\mathbf{R}\}} \hat{a}_\mathbf{R}. \quad (1)$$

Here, we introduced bosonic creation, annihilation, and number operators $\hat{a}_\mathbf{R}^\dagger$, $\hat{a}_\mathbf{R}$, and $\hat{n}_\mathbf{R} = \hat{a}_\mathbf{R}^\dagger \hat{a}_\mathbf{R}$ for site $\mathbf{R}$. We have assumed that the effects of impurities at each site are sufficiently localized that impurities at different sites contribute to separate terms in energy $E^{\{0\}} + \sum_\mathbf{R} \epsilon^{\{n_\mathbf{R}\}} n_\mathbf{R}$; i.e., long-distance interactions are negligible. We expand the

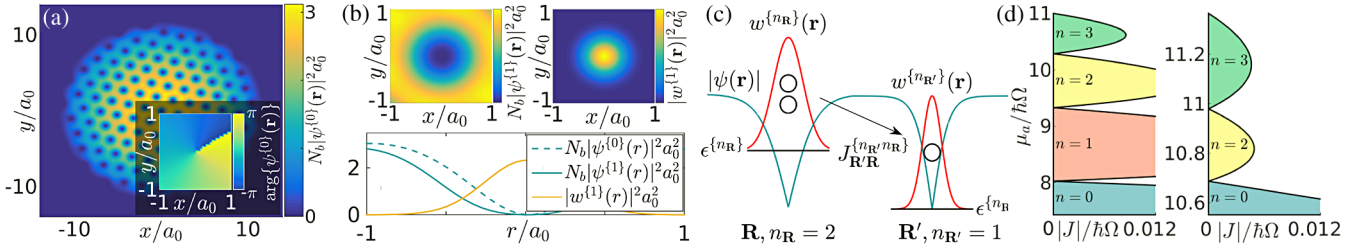


FIG. 1. Hubbard description of atoms trapped in a vortex lattice. (a) The density $N_b|\psi^{\{0\}}(\mathbf{r})|^2$ of a harmonically trapped and rotating BEC. Inset: the phase structure of the central vortex. (b) The BEC $N_b|\psi^{\{1\}}(\mathbf{r})|^2$ (top left) and impurity $|w^{\{1\}}(\mathbf{r})|^2$ (top right) densities for a single impurity localized in the central vortex. Bottom: the $x$-axis cross section of these densities, together with the unperturbed BEC density $N_b|\psi^{\{0\}}(\mathbf{r})|^2$ (dashed line). The parameters for (a) and (b) are $N_b = 500$, $\Omega/\Omega_b = 0.98$, $m_b g_b/\hbar^2 = 1$, $m_b/m_a = 1$, $g_a/g_b = 1.1$, and $g_{ab}/g_b = 6$. Quantities are expressed in terms of the characteristic length $a_0 = \sqrt{\hbar/m_b\Omega_b}$ of the trap. (c) An illustration of the Hubbard physics. Impurities at the vortex site $\mathbf{R}$ are described by the wave function $w_\mathbf{R}^{\{n_\mathbf{R}\}}(\mathbf{r})$ that, along with the deformation of the BEC wave function $|\psi(\mathbf{r})|$ in the vicinity of $\mathbf{R}$, is dependent on the occupation $n_\mathbf{R}$. This leads to an occupation-dependent energy $\epsilon^{\{n_\mathbf{R}\}}$ per impurity at the site and an occupation-dependent hopping energy $J_{\mathbf{R}'\mathbf{R}}^{\{n_{\mathbf{R}'} n_\mathbf{R}\}}$ between sites. (d) The Mott lobes (shaded regions) of the Hubbard phase diagram over different chemical potentials $\mu_a$ and hopping energies $|J|$ of the impurities, found within the Gutzwiller ansatz [62]. If $\epsilon^{\{n\}}$ increases monotonically then all Mott lobes exist; otherwise, some are missing. Here, we show both cases, corresponding to $g_a/g_b = 1.5$ and $g_{ab}/g_b = 3$ (left), and $g_a/g_b = 1.1$ and $g_{ab}/g_b = 6$ (right). The other parameters are $N_b = 10$, $m_b g_b/\hbar^2 = 1$, and $m_b/m_a = 1$.

energy per impurity $\epsilon^{\{n\}} = \epsilon^{\{1\}} + U^{\{n\}}(n-1)/2$ to define an effective single-impurity energy $\epsilon^{\{1\}}$ and two-body interaction energy $U^{\{n\}}$. A dependence of the interaction energy $U^{\{n\}}$ on the occupation $n$, often interpreted as effective three- or higher-body interactions [34], occurs when strong interactions affect the bound states of multiple impurities at a site [33–42]. Similar reasoning, applied to the hopping of particles, leads us to restrict hopping to between nearest neighbors, denoted by the angled brackets in Eq. (1), and implies that the hopping energy $J^{\{n_{\mathbf{R}'} n_{\mathbf{R}}\}}_{\mathbf{R},\mathbf{R}'}$ depends on the occupations of the sites involved.

The Hubbard model also accounts for the deformation of the BEC due to interactions with impurities [43–46]. This leads to self-trapping, where an impurity widens the vortex in which it is localized, increasing the attractiveness of the potential well for itself, lowering $\epsilon^{\{1\}}$, and other impurities, providing an effective negative contribution to the interaction energy $U^{\{n\}}$ [63]. Here, we assume the hopping $J^{\{n_{\mathbf{R}'} n_{\mathbf{R}}\}}_{\mathbf{R}'\mathbf{R}}$ is slow, allowing a simple treatment in which BEC deformations follow impurities instantaneously. Thus, for each possible configuration $\sigma = (n_{\mathbf{R}}, n_{\mathbf{R}'}, n_{\mathbf{R}''}, \ldots)$ of the impurity occupations $n_{\mathbf{R}}$ of the vortex cores, there is a single low-energy state $|\sigma\rangle$ of the system. Together these span the system's low-energy Hilbert space. Equation (1), governing the dynamics in this low-energy space, then describes polarons, quasiparticles comprising impurities and the associated vortex deformations [29–31].

We construct state $|\sigma\rangle$ in two steps. We first write it as a product $|\sigma\rangle = |\sigma; a\rangle|\sigma; b\rangle$, where the state $|\sigma; a\rangle$ of the impurities is approximately a symmetrized product of $n_{\mathbf{R}}$ impurities occupying a, potentially occupation-dependent, wave function $w^{\{n_{\mathbf{R}}\}}_{\mathbf{R}}(\mathbf{r})$ centered at each site $\mathbf{R}$. Then, the corresponding bosonic state $|\sigma; b\rangle$ is taken to be the ground state of the reduced bosonic Hamiltonian $\hat{H}_b(\sigma) = \langle\sigma; a|\hat{H}|\sigma; a\rangle$. The appropriate wave functions $w^{\{n_{\mathbf{R}}\}}_{\mathbf{R}}(\mathbf{r})$, and thus $|\sigma; a\rangle$, are found self-consistently with the deformed BEC, and thus $|\sigma; b\rangle$, by minimizing the total energy. For the regimes considered only a single minimum in the energy was observed. The parameters $\epsilon^{\{n\}}$ and $J^{\{n_{\mathbf{R}'} n_{\mathbf{R}}\}}_{\mathbf{R}'\mathbf{R}}$ of the Hubbard Hamiltonian $\hat{H}_{\text{Hubbard}}$ [Eq. (1)] are then chosen such that they reproduce the action of the original Hamiltonian in this low-energy subspace $\langle\sigma'|\hat{H}_{\text{Hubbard}}|\sigma\rangle = \langle\sigma'|\hat{H}|\sigma\rangle$. For calculation details, see Secs. II and III of the Supplemental Material [56].

*Weak interactions.*—We first consider the limit in which, due to weak interactions, impurities and deformations of the vortex lattice do not affect each other [29]. In this case, the correct impurity wave functions are the localized lowest-band Wannier modes $w_{\mathbf{R}}(\mathbf{r})$ for the vortex lattice potential $V^{\{0\}}_{ab}(\mathbf{r})$ formed by the unperturbed condensate $\psi^{\{0\}}(\mathbf{r})$. Note that the Wannier modes do not depend on occupation. We then calculate $|\sigma; b\rangle$ within a Bogoliubov approximation of the BEC. Specifically, we write $\hat{\Psi}_b(\mathbf{r}) = \sqrt{N_b}\psi^{\{0\}}(\mathbf{r}) + \delta\hat{\Psi}_b(\mathbf{r})$ with the deformation $\delta\hat{\Psi}_b(\mathbf{r}) = \sum_{\mathbf{k}}[u_{\mathbf{k}}(\mathbf{r})\hat{b}_{\mathbf{k}} + v^*_{\mathbf{k}}(\mathbf{r})\hat{b}^\dagger_{\mathbf{k}}]$ expressed in terms of bosonic operators $\hat{b}^\dagger_{\mathbf{k}}$ and $\hat{b}_{\mathbf{k}}$, and $u_{\mathbf{k}}(\mathbf{r})$ and $v_{\mathbf{k}}(\mathbf{r})$ satisfying the Bogoliubov–de Gennes equations for mode energies $\hbar\omega_{\mathbf{k}}$ [64]. Including terms up to second order in $\delta\hat{\Psi}_b(\mathbf{r})$ and $g_{ab}$, and neglecting hopping induced by impurity-impurity interactions, we obtain the reduced bosonic Hamiltonian

$$\hat{H}_b(\sigma) = E_b[\psi^{\{0\}}] + \sum_{\mathbf{k}} \hbar\omega_{\mathbf{k}} \hat{b}^\dagger_{\mathbf{k}} \hat{b}_{\mathbf{k}} + g_{ab} \sum_{\mathbf{k}} (f_{\mathbf{k}} \hat{b}_{\mathbf{k}} + f^*_{\mathbf{k}} \hat{b}^\dagger_{\mathbf{k}})$$

with $f_{\mathbf{k}} = \sum_{\mathbf{R}} n_{\mathbf{R}} f_{\mathbf{k}\mathbf{R}}$, $f_{\mathbf{k}\mathbf{R}} = \int d\mathbf{r} |w_{\mathbf{R}}(\mathbf{r})|^2 f_{\mathbf{k}}(\mathbf{r})$, and $f_{\mathbf{k}}(\mathbf{r}) = \sqrt{N_b}[u_{\mathbf{k}}(\mathbf{r})\psi^{\{0\}*}(\mathbf{r}) + v_{\mathbf{k}}(\mathbf{r})\psi^{\{0\}}(\mathbf{r})]$. The constant $E_b[\psi^{\{0\}}]$ is the energy of the unperturbed condensate. The ground state of $\hat{H}_b(\sigma)$ is the displaced phonon vacuum $|\sigma; b\rangle = \prod_{\mathbf{R}} (\hat{X}^\dagger_{\mathbf{R}})^{n_{\mathbf{R}}} |0\rangle$, where $\hat{X}^\dagger_{\mathbf{R}} = \exp[\sum_{\mathbf{k}} (\alpha^*_{\mathbf{k}\mathbf{R}} \hat{b}^\dagger_{\mathbf{k}} - \alpha_{\mathbf{k}\mathbf{R}} \hat{b}_{\mathbf{k}})]$ is a Glauber displacement operator with $\alpha_{\mathbf{k}\mathbf{R}} = -g_{ab} f_{\mathbf{k}\mathbf{R}}/\hbar\omega_{\mathbf{k}}$.

We then find (see Sec. II of the Supplemental Material [56]) the parameters of the Hubbard Hamiltonian $\hat{H}_{\text{Hubbard}}$ [Eq. (1)] to be the following. The zero energy is $E^{\{0\}} = E_b[\psi^{\{0\}}]$, while the on-site energy per impurity $\epsilon^{\{1\}} = \varepsilon - V$ consists of the contribution $\varepsilon = \int d\mathbf{r} w^*_{\mathbf{R}}(\mathbf{r})[h_a(\mathbf{r}) + V^{\{0\}}_{ab}(\mathbf{r})] w_{\mathbf{R}}(\mathbf{r})$ from an impurity in the unperturbed potential, reduced by an energy $V = g^2_{ab} \sum_{\mathbf{k}} |\int d\mathbf{r} |w_{\mathbf{R}}(\mathbf{r})|^2 f_{\mathbf{k}}(\mathbf{r})|^2/\hbar\omega_{\mathbf{k}}$ due to self-trapping via BEC deformation. The two-particle interaction $U = u - 2V$ consists of the usual contribution $u = g_a \int d\mathbf{r} |w_{\mathbf{R}}(\mathbf{r})|^4$ for the impurity reduced by twice the self-trapping energy $V$. The hopping $J_{\mathbf{R}'\mathbf{R}} = \langle 0|\hat{X}_{\mathbf{R}'}\hat{X}^\dagger_{\mathbf{R}}|0\rangle j_{\mathbf{R}'\mathbf{R}}$ is reduced from the bare impurity hopping $j_{\mathbf{R}'\mathbf{R}} = \int d\mathbf{r} w^*_{\mathbf{R}'}(\mathbf{r})[h_a(\mathbf{r}) + V^{\{0\}}_{ab}(\mathbf{r})] w_{\mathbf{R}}(\mathbf{r})$ by a renormalization factor $\langle 0|\hat{X}_{\mathbf{R}'}\hat{X}^\dagger_{\mathbf{R}}|0\rangle$ resulting again from BEC deformation. The polaron creation and annihilation operators are simply expressed as $\hat{a}^\dagger_{\mathbf{R}} = (\int d\mathbf{r} w_{\mathbf{R}}(\mathbf{r}) \hat{\Psi}^\dagger_a(\mathbf{r})) \hat{X}^\dagger_{\mathbf{R}}$ and its conjugate; i.e., a polaron consists of an impurity with the Wannier function $w_{\mathbf{R}}(\mathbf{r})$ dressed with a corresponding displacement $\hat{X}^\dagger_{\mathbf{R}}$ of the BEC [29].

This calculation finds the competing contributions of both the direct interaction $u$ and self-trapping $V$ to be occupation independent. Thus, the energy per impurity $\epsilon^{\{n\}}$ exhibits only two possible behaviors: monotonically decreasing with $n$ (attractive $U < 0$), in which no Mott phases exist, or monotonically increasing with $n$ (repulsive $U > 0$), leading to the usual Mott phase diagram, as on the left of Fig. 1(d). Treating the deformation of the BEC in a Thomas-Fermi approximation [25], we find the approximate condition $g_{ab} > \sqrt{g_a g_b/2}$ for the onset of negative $U$.

*Strong interactions.*—In this regime, the state of multiple impurities localized at the same site can no longer be

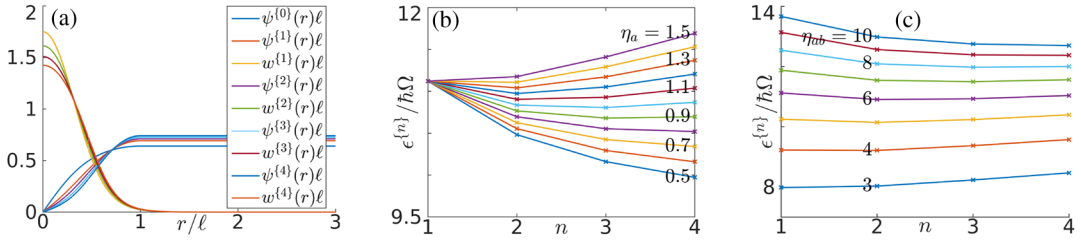


FIG. 2. Strong coupling. (a) The BEC wave function $|\psi^{\{n\}}(r)|$, normalized over the unit cell $0 \le r \le \ell$, and the impurity wave function $w^{\{n\}}(r)$, normalized over all space, for different numbers of impurities $n$. The energy per impurity $\epsilon^{\{n\}}$, for different $n$, as (b) $\eta_a = g_a/g_b$ and (c) $\eta_{ab} = g_{ab}/g_b$ is varied. Crosses mark data points and lines guide the eye. Unless stated otherwise, $N_b = 10$ is the number of bosons per unit cell, $m_b g_b/\hbar^2 = 1$, $m_b/m_a = 1$, $g_a/g_b = 1.1$, and $g_{ab}/g_b = 6$.

described in terms of the lowest-band Wannier functions $w_{\mathbf{R}}(\mathbf{r})$. To account for the effect of higher bands in our single-band model, we thus require occupation-dependent wave functions $w_{\mathbf{R}}^{\{n_{\mathbf{R}}\}}(\mathbf{r})$ to describe the impurities at each site $\mathbf{R}$ [38,65–67]. Similarly, to describe the condensate in the vicinity of the site, we use an occupation-dependent wave function $\psi_{\mathbf{R}}^{\{n_{\mathbf{R}}\}}(\mathbf{r})$. The self-consistent wave functions $w_{\mathbf{R}}^{\{n_{\mathbf{R}}\}}(\mathbf{r})$ and $\psi_{\mathbf{R}}^{\{n_{\mathbf{R}}\}}(\mathbf{r})$ that optimally describe the low-energy manifold are those that simultaneously minimize the energy at the site. Omitting the site label, the energy functional to minimize is (see Sec. III of the Supplemental Material [56])

$$\begin{aligned} E^{\{0\}} + \epsilon^{\{n\}} n = {} & n \int d\mathbf{r} w^{\{n\}*}(\mathbf{r}) h_a(\mathbf{r}) w^{\{n\}}(\mathbf{r}) \\ & + \frac{g_a n(n-1)}{2} \int d\mathbf{r} |w^{\{n\}}(\mathbf{r})|^4 \\ & + N_b \int d\mathbf{r} \psi^{\{n\}*}(\mathbf{r}) h_b(\mathbf{r}) \psi^{\{n\}}(\mathbf{r}) \\ & + \frac{g_b}{2} N_b^2 \int d\mathbf{r} |\psi^{\{n\}}(\mathbf{r})|^4 \\ & + n N_b g_{ab} \int d\mathbf{r} |w^{\{n\}}(\mathbf{r})|^2 |\psi^{\{n\}}(\mathbf{r})|^2, \end{aligned}$$

for each $n$, with $E^{\{0\}}$ and $\epsilon^{\{n\}}$ determined from the energies at the minima.

We perform the energy minimization over the unit cell corresponding to some site $\mathbf{R}$ in the bulk, approximating it by a circular region of radius $\ell = \sqrt{\hbar/m_b\Omega}$ and area equal to that of the unit cell (see Sec. IV of the Supplemental Material [56]). We fix the number $N_b$ of bosons in a unit cell and use a Crank-Nicolson finite-difference approach [68]. We account for the BEC rotation and trapping by making two assumptions: first, that the BEC wave function has a simple angular dependence $\psi^{\{n\}}(\mathbf{r}) = e^{i\phi}\psi^{\{n\}}(r)$ inside the unit cell [Fig. 1(a)]; second, that the wave function $\psi^{\{n\}}(r)$ takes its maximum value at the boundary of the cell [Fig. 1(b)]. We also assume no angular dependence for the impurity wave function $w^{\{n\}}(\mathbf{r}) = w^{\{n\}}(r)$.

The results are shown in Fig. 2. In Fig. 2(a) we observe the widening of both the impurity wave function and vortex core due to strong interactions. In Figs. 2(b) and 2(c) we plot the occupation dependence of the energy per impurity $\epsilon^{\{n\}}$ for varying intra- and interspecies interaction strengths $g_a$ and $g_{ab}$. We see that the competing effects of direct repulsive interactions and attractive mediated interactions are separately occupation dependent. Specifically, the effect of self-trapping decreases quickly with occupation due to the reduced effect of an impurity on a vortex core that has already been widened. Direct interactions, meanwhile, remain important for larger $n$. Thus, we find regimes in which $U^{\{n\}}$ is initially negative and then positive, and $\epsilon^{\{n\}}$ is nonmonotonic, first decreasing then increasing.

This corresponds to unusual behavior in the phase diagram, which we calculate within the Gutzwiller ansatz [62] for two sets of parameters, assuming the hopping to have a constant magnitude $|J|$ (see Sec. V of the Supplemental Material [56]). The Mott lobes, up to $n = 3$, are shown in Fig. 1(d). We see that as the strength of impurity-BEC interactions $g_{ab}$ increases relative to impurity-impurity interactions $g_a$, the $n = 1$ Mott lobe disappears completely.

*Hopping.*—While the chemical potential $\mu_a$ of the impurity can be controlled independently, the magnitude $|J|$ of the hopping depends on the other parameters. Here, we estimate the magnitude $|J|$, demonstrating that we are in the region of the phase diagram containing the Mott lobes and validating our earlier assumption of slow hopping. We take two of the previously calculated single-impurity wave functions $w_{\mathbf{R}}^{\{1\}}(\mathbf{r})$, located at neighboring sites $\mathbf{R}$ and $\mathbf{R}'$, orthogonalize them (see Sec. VI of the Supplemental Material [56]), and calculate the bare hopping using the unperturbed potential $j_{\mathbf{R}'\mathbf{R}} = \int d\mathbf{r} w_{\mathbf{R}'}^{\{1\}*}(\mathbf{r})[h_a(\mathbf{r}) + V_{ab}^{\{0\}}(\mathbf{r})]w_{\mathbf{R}}^{\{1\}}(\mathbf{r})$. For the parameters $N_b = 10$, $m_b g_b/\hbar^2 = 1$, $m_b/m_a = 1$, and $g_{ab}/g_b = 6$, corresponding to the missing Mott lobe, we find $|j_{\mathbf{R}'\mathbf{R}}| = 7.4 \times 10^{-3}\hbar\Omega$. The true magnitude $|J_{\mathbf{R}'\mathbf{R}}^{\{n_{\mathbf{R}'}n_{\mathbf{R}}\}}|$ of the hopping energies will be renormalized to a significantly smaller value than this due to deformations of the BEC. Hopping is thus the smallest energy scale in our system, 1 order of magnitude below $U^{\{n\}}$.

*Discussion.*—We have shown that it is possible to trap cold atomic impurities in the vortex lattice formed by

rotating bosons of another species, have described their motion by a Hubbard model, and have shown that the Mott lobes of the resulting phase diagram have unusual features. Such features, including missing Mott lobes, can be observed in experiment, inferred from time-of-flight imaging [69,70] since the lattice parameter $a$ is smaller than the wavelength of light. To confirm the feasibility of this, note that the energy scale of the system is determined by the rotation and trapping frequencies $\Omega \approx \Omega_s$, which can be on the order of 100 Hz in magnetic traps and 1 kHz in dipole traps. For example, $\Omega/2\pi = 3$ kHz is equivalent to $\hbar\Omega/k_B = 150$ nK. The temperature needs to be less than $0.2\hbar\Omega/k_B = 30$ nK to distinguish the Mott lobes, as is evident from Fig. 1(d), which is experimentally achievable. We note that our calculations neglect correlations between particles at the same site, which for strong interactions may lead to a significant reduction in the on-site energies [39] and enhance the occupation-dependent interaction effects.

As well as the strongly interacting region of the phase diagram and the Mott lobes on which we have focused, strong interactions significantly affect other phases, including inducing a superfluid of paired impurities [38]. Indeed, for highly mobile impurities effects such as bistability and hysteresis may arise. Moreover, the interplay of incoherent polaronic effects, e.g., motional dephasing [28–30], and vortices is an interesting prospect for future work. While we have focused on bosonic impurities, fermions could also be considered in the same framework where novel vortex induced pairing effects are expected to arise.

T. H. J. and D. J. thank the National Research Foundation and the Ministry of Education of Singapore for support. W. B. thanks the Ministry of Education of Singapore for support through Grant No. R-146-000-196-112. The research leading to these results has received funding from the European Research Council under the European Union's Seventh Framework Programme (FP7/2007-2013) Grant Agreement No. 319286 Q-MAC and the collaborative project QuProCS Grant Agreement No. 641277 under H2020-EU.1.2.2.–FET Proactive. We gratefully acknowledge financial support from the Oxford Martin School Programme on Bio-Inspired Quantum Technologies.

*matbaowz@nus.edu.sg
†s.r.clark@bath.ac.uk

[1] A. G. Cade, Phys. Rev. Lett. **15**, 238 (1965).
[2] R. L. Douglass, Phys. Rev. **141**, 192 (1966).
[3] W. P. Pratt and W. Zimmermann, Phys. Rev. **177**, 412 (1969).
[4] G. Gamota, J. Phys. Colloques **31**, C3-39 (1970).
[5] R. E. Packard and T. M. Sanders, Phys. Rev. Lett. **22**, 823 (1969).
[6] G. A. Williams and R. E. Packard, Phys. Rev. Lett. **33**, 280 (1974).
[7] G. P. Bewley, D. P. Lathrop, and K. R. Sreenivasan, Nature (London) **441**, 588 (2006).
[8] L. F. Gomez, K. R. Ferguson, J. P. Cryan, C. Bacellar, R. M. P. Tanyag, C. Jones, S. Schorb, D. Anielski, A. Belkacem, C. Bernando *et al.*, Science **345**, 906 (2014).
[9] R. L. Douglass, Phys. Rev. **174**, 255 (1968).
[10] W. I. Glaberson, D. M. Strayer, and R. J. Donnelly, Phys. Rev. Lett. **21**, 1740 (1968).
[11] J. E. Sonier, J. H. Brewer, and R. F. Kiefl, Rev. Mod. Phys. **72**, 769 (2000).
[12] C. Caroli, P. D. Gennes, and J. Matricon, Phys. Lett. **9**, 307 (1964).
[13] L. Kramer and W. Pesch, Z. Phys. **269**, 59 (1974).
[14] F. Gygi and M. Schlüter, Phys. Rev. B **43**, 7609 (1991).
[15] H. F. Hess, R. B. Robinson, R. C. Dynes, J. M. Valles, and J. V. Waszczak, Phys. Rev. Lett. **62**, 214 (1989).
[16] D. Rainer, J. A. Sauls, and D. Waxman, Phys. Rev. B **54**, 10094 (1996).
[17] J. Abo-Shaeer, C. Raman, J. Vogels, and W. Ketterle, Science **292**, 476 (2001).
[18] K. W. Madison, F. Chevy, W. Wohlleben, and J. Dalibard, Phys. Rev. Lett. **84**, 806 (2000).
[19] V. Schweikhard, I. Coddington, P. Engels, V. P. Mogendorff, and E. A. Cornell, Phys. Rev. Lett. **92**, 040404 (2004).
[20] R. A. Williams, S. Al-Assam, and C. J. Foot, Phys. Rev. Lett. **104**, 050404 (2010).
[21] A. L. Fetter, Rev. Mod. Phys. **81**, 647 (2009).
[22] S. Palzer, C. Zipkes, C. Sias, and M. Köhl, Phys. Rev. Lett. **103**, 150601 (2009).
[23] C. J. Mathy, M. B. Zvonarev, and E. Demler, Nat. Phys. **8**, 881 (2012).
[24] J. Catani, G. Lamporesi, D. Naik, M. Gring, M. Inguscio, F. Minardi, A. Kantian, and T. Giamarchi, Phys. Rev. A **85**, 023623 (2012).
[25] T. H. Johnson, M. Bruderer, Y. Cai, S. R. Clark, W. Bao, and D. Jaksch, Europhys. Lett. **98**, 26001 (2012).
[26] A. V. Ponomarev, J. Madroñero, A. R. Kolovsky, and A. Buchleitner, Phys. Rev. Lett. **96**, 050404 (2006).
[27] M. Bruderer, T. H. Johnson, S. R. Clark, D. Jaksch, A. Posazhennikova, and W. Belzig, Phys. Rev. A **82**, 043617 (2010).
[28] T. H. Johnson, S. R. Clark, M. Bruderer, and D. Jaksch, Phys. Rev. A **84**, 023617 (2011).
[29] M. Bruderer, A. Klein, S. R. Clark, and D. Jaksch, Phys. Rev. A **76**, 011605 (2007).
[30] A. Klein, M. Bruderer, S. R. Clark, and D. Jaksch, New J. Phys. **9**, 411 (2007).
[31] A. Schirotzek, C.-H. Wu, A. Sommer, and M. W. Zwierlein, Phys. Rev. Lett. **102**, 230402 (2009).
[32] M. A. Caracanhas, V. S. Bagnato, and R. G. Pereira, Phys. Rev. Lett. **111**, 115304 (2013).
[33] J. Li, Y. Yu, A. M. Dudarev, and Q. Niu, New J. Phys. **8**, 154 (2006).
[34] P. R. Johnson, E. Tiesinga, J. V. Porto, and C. J. Williams, New J. Phys. **11**, 093022 (2009).
[35] K. R. A. Hazzard and E. J. Mueller, Phys. Rev. A **81**, 031602 (2010).
[36] H. P. Büchler, Phys. Rev. Lett. **104**, 090402 (2010).
[37] H. P. Büchler, Phys. Rev. Lett. **108**, 069903(E) (2012).
[38] O. Dutta, A. Eckardt, P. Hauke, B. Malomed, and M. Lewenstein, New J. Phys. **13**, 023019 (2011).

[39] U. Bissbort, F. Deuretzbacher, and W. Hofstetter, Phys. Rev. A **86**, 023617 (2012).
[40] D.-S. Lühmann, O. Jürgensen, and K. Sengstock, New J. Phys. **14**, 033021 (2012).
[41] M. Łacki, D. Delande, and J. Zakrzewski, New J. Phys. **15**, 013062 (2013).
[42] J. Major, M. Łacki, and J. Zakrzewski, Phys. Rev. A **89**, 043626 (2014).
[43] D.-S. Lühmann, K. Bongs, K. Sengstock, and D. Pfannkuche, Phys. Rev. Lett. **101**, 050402 (2008).
[44] R. M. Lutchyn, S. Tewari, and S. Das Sarma, Phys. Rev. A **79**, 011606 (2009).
[45] A. Mering and M. Fleischhauer, Phys. Rev. A **83**, 063630 (2011).
[46] O. Jürgensen, K. Sengstock, and D.-S. Lühmann, Phys. Rev. A **86**, 043623 (2012).
[47] O. Dutta, M. Gajda, P. Hauke, M. Lewenstein, D.-S. Lühmann, B. A. Malomed, T. Sowiński, and J. Zakrzewski, Rep. Prog. Phys. **78**, 066001 (2015).
[48] J. Hirsch, Physica (Amsterdam) **158C**, 326 (1989).
[49] R. Strack and D. Vollhardt, Phys. Rev. Lett. **70**, 2637 (1993).
[50] J. Hirsch, Physica (Amsterdam) **199B–200B**, 366 (1994).
[51] J. C. Amadon and J. E. Hirsch, Phys. Rev. B **54**, 6364 (1996).
[52] S. Kaiser, S. R. Clark, D. Nicoletti, G. Cotugno, R. Tobey, N. Dean, S. Lupi, H. Okamoto, T. Hasegawa, D. Jaksch *et al.*, Sci. Rep. **4**, 3823 (2014).
[53] J. Larson, B. Damski, G. Morigi, and M. Lewenstein, Phys. Rev. Lett. **100**, 050401 (2008).
[54] F. Brennecke, T. Donner, S. Ritter, T. Bourdel, M. Kohl, and T. Esslinger, Nature (London) **450**, 268 (2007).
[55] G. Szirmai, D. Nagy, and P. Domokos, Phys. Rev. Lett. **102**, 080401 (2009).
[56] See Supplemental Material at http://link.aps.org/supplemental/10.1103/PhysRevLett.116.240402 for additional details regarding the methods and calculations described in the main text, which includes Refs. [71–73].
[57] W. Bao and Q. Du, SIAM J. Sci. Comput. **25**, 1674 (2004).
[58] W. Bao, I.-L. Chern, and F. Y. Lim, J. Comput. Phys. **219**, 836 (2006).
[59] W. Bao and Y. Cai, Kinet. Relat. Models **6**, 1 (2013).
[60] N. R. Cooper, N. K. Wilkin, and J. M. F. Gunn, Phys. Rev. Lett. **87**, 120405 (2001).
[61] G. Baym, J. Low Temp. Phys. **138**, 601 (2005).
[62] R. O. Umucalilar and M. O. Oktel, Phys. Rev. A **76**, 055601 (2007).
[63] M. Bruderer, W. Bao, and D. Jaksch, Europhys. Lett. **82**, 30004 (2008).
[64] P. Öhberg, E. L. Surkov, I. Tittonen, S. Stenholm, M. Wilkens, and G. V. Shlyapnikov, Phys. Rev. A **56**, R3346 (1997).
[65] M. Chiofalo, M. Polini, and M. Tosi, Eur. Phys. J. D **11**, 371 (2000).
[66] P. Vignolo, Z. Akdeniz, and M. P. Tosi, J. Phys. B **36**, 4535 (2003).
[67] J.-F. Schaff, Z. Akdeniz, and P. Vignolo, Phys. Rev. A **81**, 041604 (2010).
[68] S. K. Adhikari, Phys. Rev. E **62**, 2937 (2000).
[69] M. Greiner, O. Mandel, T. Esslinger, T. W. Hänsch, and I. Bloch, Nature (London) **415**, 39 (2002).
[70] S. Fölling, F. Gerbier, A. Widera, O. Mandel, T. Gericke, and I. Bloch, Nature (London) **434**, 481 (2005).
[71] R. Walters, G. Cotugno, T. H. Johnson, S. R. Clark, and D. Jaksch, Phys. Rev. A **87**, 043613 (2013).
[72] R. Bhat, B. M. Peden, B. T. Seaman, M. Krämer, L. D. Carr, and M. J. Holland, Phys. Rev. A **74**, 063606 (2006).
[73] R. Bhat, M. Krämer, J. Cooper, and M. J. Holland, Phys. Rev. A **76**, 043601 (2007).